JACC: BASIC TO TRANSLATIONAL SCIENCE VOL. 8, NO. 1, 2023

ORIGINAL RESEARCH - CLINICAL

Spatial Distribution of Calcium Sparks Determines Their Ability to Induce Afterdepolarizations in Human Atrial Myocytes

Carmen Tarifa, PhD,[a,b] Alexander Vallmitjana, PhD,[c] Verónica Jiménez-Sábado, PhD,[a,b,d] Miquel Marchena, PhD,[e] Anna Llach, PhD,[b] Adela Herraiz-Martínez, PhD,[a,b] Héctor Godoy-Marín, PhD,[f,g] Carme Nolla-Colomer, PhD,[c] Antonino Ginel, MD,[h] Xavier Viñolas, MD,[i] José Montiel, MD,[h] Francisco Ciruela, PhD,[f,g] Blas Echebarria, PhD,[e] Raúl Benítez, PhD,[c] Juan Cinca, MD,[b,d,i] Leif Hove-Madsen, PhD[a,b,d]

VISUAL ABSTRACT

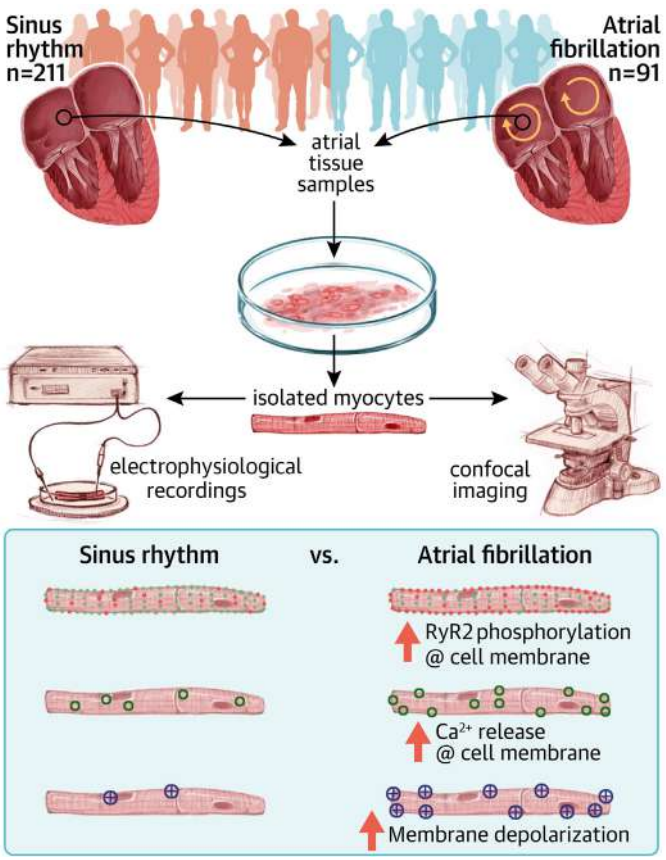

Tarifa C, et al. J Am Coll Cardiol Basic Trans Science. 2023;8(1):1-15.

HIGHLIGHTS

- A newly developed analysis methodology uncovers a preferential increase in calcium sparks near the sarcolemma in myocytes from patients with AF, which is linked to higher ryanodine receptor (RyR2) phosphorylation at s2808 and lower calsequestrin-2 levels.
- A novel mathematical human atrial myocyte model, incorporating modulation of RyR2 gating, shows that only the observed combination of changes in RyR2 phosphorylation and calsequestrin-2 levels can account for the shift in the spatio-temporal distribution of sparks in patients with AF.
- Preferential calcium release near the sarcolemma is the key to a higher incidence and amplitude of afterdepolarizations in atrial myocytes from patients with AF.

ISSN 2452-302X https://doi.org/10.1016/j.jacbts.2022.07.013

ABBREVIATIONS AND ACRONYMS

AF = atrial fibrillation

Csq-2 = cardiac calsequestrin (type 2)

I_{Ca} = calcium current

I_{TI} = transient inward current

NCX-1 = cardiac Na^+/Ca^{2+} exchanger (type 1)

PLB = phospholamban

RyR2 = cardiac ryanodine receptor (type 2)

SERCA2a = cardiac sarcoplasmic reticulum Ca-ATPase pump protein (type 2)

SR = sarcoplasmic reticulum

SUMMARY

Analysis of the spatio-temporal distribution of calcium sparks showed a preferential increase in sparks near the sarcolemma in atrial myocytes from patients with atrial fibrillation (AF), linked to higher ryanodine receptor (RyR2) phosphorylation at s2808 and lower calsequestrin-2 levels. Mathematical modeling, incorporating modulation of RyR2 gating, showed that only the observed combinations of RyR2 phosphorylation and calsequestrin-2 levels can account for the spatio-temporal distribution of sparks in patients with and without AF. Furthermore, we demonstrate that preferential calcium release near the sarcolemma is key to a higher incidence and amplitude of afterdepolarizations in atrial myocytes from patients with AF.

Atrial fibrillation (AF) has been associated with changes in the expression or activity of calcium handling proteins.[1-5] These include alterations in the L-type calcium current (I_{Ca}) density,[2,3] sarcoplasmic reticulum (SR) calcium uptake,[6] and spontaneous SR calcium release[1] through the RyR2. This, in turn, activates the cardiac Na^+/Ca^{2+} exchanger (type 1) (NCX-1), giving rise to concurrent transient inward currents (I_{TI}), membrane depolarizations[5,7-9] and cellular arrhythmia.[10]

A common mechanism proposed to explain the remodeling of the activity of calcium regulatory proteins is a change in their phosphorylation state.[4,7,9,11-13] Reported modulations of calcium handling proteins in AF include increased phosphorylation of the RyR2 at s2808,[4,14] and a calmodulin kinase II-dependent phosphorylation of the RyR2 at s2814.[5,13] Similarly, protein kinase A-dependent phosphorylation of phospholamban (PLB) at ser-16 or calmodulin kinase II-dependent phosphorylation of PLB at thr-17 has been shown to modulate SR calcium uptake through regulation of cardiac SR Ca-ATPase pump protein (type 2) (SERCA2a) activity.[7,13] All of these mechanisms have been claimed to promote atrial arrhythmia by increasing the frequency of local calcium release events (calcium sparks), which in turn may favor the induction of spontaneous calcium waves[1] and membrane depolarizations large enough to trigger atrial arrhythmic episodes.[8,9]

Interestingly, a higher incidence of spontaneous calcium release events may not be arrhythmogenic if they are unable to induce membrane depolarizations large enough to induce arrhythmia.[15] In this regard, it is unclear why calcium waves give rise to small afterdepolarizations in myocytes from patients without AF while calcium waves of a similar magnitude give rise to large afterdepolarizations or spontaneous action potentials in atrial myocytes from patients with AF.[5] Higher NCX-1 expression has been proposed as an underlying mechanism,[5] but reports on NCX-1 expression and activity in AF vary.[1,5,16,17] Furthermore, increased RyR2 phosphorylation in AF is expected to lower the threshold for spontaneous calcium release, and this is expected to reduce the SR calcium content.[18] Persistent or permanent AF has been associated with unchanged or reduced SR calcium content[1,5,13] and unchanged or smaller calcium spark amplitude,[19] which, in turn, would tend to reduce the amplitude of afterdepolarizations. An alternative and novel hypothesis is that the induction of larger afterdepolarizations in AF is caused by a differential increase in spontaneous calcium release near the NCX-1, induced by activation of Gs-protein coupled receptors, and favored by the relative paucity of t-tubules in human atrial myocytes.[10,20,21]

From the [a]Instituto de Investigaciones Biomédicas de Barcelona, IIBB-CSIC, Barcelona, Spain; [b]IIB Sant Pau, Hospital de la Santa Creu i Sant Pau, Barcelona, Spain; [c]Department d'Enginyeria de Sistemes, Automàtica i Informàtica Industrial, Universitat Politècnica de Catalunya, Spain; [d]Centro de Investigación Biomédica en Red Enfermedades Cardiovaculares, Madrid, Spain; [e]Department Physics, Universitat Politècnica de Catalunya, Barcelona, Spain; [f]Department Pathology and Experimental Therapeutics, IDIBELL, University of Barcelona, Barcelona, Spain; [g]Neuroscience Institute, University of Barcelona, Barcelona, Spain; [h]Servicio de Cirugía Cardiaca, Hospital de la Santa Creu i Sant Pau, Barcelona, Spain; and the [i]Servicio de Cardiología, Hospital de la Santa Creu i Sant Pau, Barcelona, Spain.

The authors attest they are in compliance with human studies committees and animal welfare regulations of the authors' institutions and Food and Drug Administration guidelines, including patient consent where appropriate. For more information, visit the Author Center.

Manuscript received January 21, 2022; revised manuscript received July 18, 2022, accepted July 18, 2022.

This would increase the amount of calcium extruded by the NCX-1, increasing the I_{TI} amplitude, and give rise to a larger afterdepolarization. We have previously reported subcellular differences in calcium transient dynamics in human atrial myocytes,[10,21] but because most calcium imaging studies use confocal line-scan imaging, little attention has been paid to pathological alterations in the calcium spark distribution and the resulting functional impact.

Therefore, to test the hypothesis that AF is associated with a differential increase in calcium release near the sarcolemma, which is the key to large and frequent afterdepolarizations in patients with this arrhythmia, we here aimed to investigate the functional impact of AF on the spatio-temporal alterations in the distribution of calcium sparks in these patients and to identify the underlying molecular mechanisms.

METHODS

MYOCYTE ISOLATION. Right atrial samples from 302 patients undergoing cardiac surgery were used for myocyte isolation and different experimental protocols as detailed in the Supplemental Methods. Patients were divided into 2 groups according to the presence or absence of AF. Clinical characteristics, sex, echocardiographic data, and pharmacological treatments of patients are summarized in Supplemental Table 1. The table also specifies the number of patients with AF who had paroxysmal vs persistent or permanent AF. All patients gave informed written consent to obtain biological samples, and the Ethics Committee of our institution approved the study protocol (protocol code: AZAR-AF_2015). The investigation conforms to the principles outlined in the Declaration of Helsinki.

PATCH-CLAMP TECHNIQUE. Recordings of I_{TI} currents and caffeine-induced NCX-1 current were done using the perforated patch-clamp technique as previously described[10,16] and detailed in the Supplemental Methods. Current-clamp configuration using K^+-containing intracellular and extracellular media was used to detect spontaneous membrane depolarizations and action potentials as described in the Supplemental Methods.

PROTEIN EXPRESSION AND DISTRIBUTION. Protein expression was determined using western blotting as described in the Supplemental Methods. To visualize cardiac calsequestrin (type 2) (Csq-2), total RyR2, and s2808 or s2814 phosphorylated RyR2, isolated myocytes were fixed with 5% paraformaldehyde for 10 minutes at room temperature. Subsequently, cells were incubated with phosphate-buffered saline (PBS)/glycine 0.1 mol/L for 10 minutes and thereafter with PBS/0.2% Triton X-100 for at least 15 minutes to permeabilize the cells. To block the nonspecific sites, the cells were incubated with PBS/0.2% Tween 20 and 10% horse serum for 30 minutes. Total s2808 or s2814 phosphorylated RyR2 was labeled with the primary antibodies mouse anti-RyR2 (C3-33 NR07, 1:1,200, Calbiochem), rabbit anti-s2808-P (1:1,200, A010-30, Badrilla), or rabbit anti-s2814-P (1:1,200, A010-31, Badrilla). Csq-2 and voltage-gated L-type calcium channel (Cav1.2) were labeled with primary rabbit anti-Csq-2 (1:500, Ab-3516, Abcam) and guinea pig anti-Cav1.2 (1:600, AGP-001, Alomone) antibodies, respectively. These secondary antibodies, AlexaFluor 488 antimouse (diluted 1:2,000), AlexaFluor 594 antirabbit (diluted 1:1,500), and AlexaFluor 594 anti-guinea pig (diluted 1:1,000) were used to stain total RyR2 (in green) and s2808 phosphorylated RyR2, s2814 phosphorylated RyR2, Csq-2, or Cav1.2 (in red). Images were acquired with a confocal microscope (Leica AOBS SP5) and a 63× glycerol immersion objective.

DETECTION AND CHARACTERIZATION OF CALCIUM SPARKS. To analyze the properties, spatial distribution, and frequency of the calcium sparks, human atrial myocytes were loaded with a calcium-sensitive dye (fluo-4 or Cal-520) as previously described,[19] and images (140 × 512 pixels) were recorded at a frame rate of 90 Hz. Calcium sparks were detected using a custom-made image processing and analysis pipeline of live cell imaging data (SparkSimple). This tool identifies potential calcium spark candidates, their properties, and spatio-temporal distribution, followed by filtering delimiting the calcium spark dimensions as well as the minimal temporal and spatial distance between sparks (see Supplemental Methods for details). Subsequently, accepted sparks occurring repeatedly in the same place were pooled into a single spark site, allowing determination of the site density and the spark frequency per site. Supplemental Figure 1A shows an example of a human atrial myocyte with the detection of 6 sparks located in 2 spark sites (left). Recordings of the calcium signal in each of the 2 spark sites are shown in the middle panel, and one of the sparks is shown on the right together with the key features determined by the detection algorithm. To determine the impact of the signal-to-noise ratio on spark detection, we used a mathematical myocyte model (see the following text) to generate synthetic sparks and determine the impact of signal noise on spark detection and properties. The algorithm successfully detected sparks with signal-to-noise ratios (signal/[max noise − min noise]/2) higher than 2.62 ± 0.15 (Supplemental Figure 1B). To

fine-tune the filtering parameters of the algorithm in human atrial myocytes, all sparks identified by the program were inspected manually and accepted or rejected as valid sparks using a validation subroutine within the detection program developed for this purpose. Supplemental Figure 1C summarizes the features of 3,342 validated sparks in atrial myocytes from 79 patients. The spark amplitude (amp) had an asymmetric distribution because small-amplitude events, including sparks above or below the confocal plane, were discarded by the filter settings. Similarly, potential events with very fast decay (tau) could not be distinguished from noise and were eliminated by the detection filter. The Spark-Simple algorithms are available in Matlab format online.[22]

MATHEMATICAL MODEL. To study the effects of spatial gradients in RyR2 phosphorylation and Csq-2 levels on RyR2 activity we developed a new mathematical model of calcium dynamics in human atrial myocytes, based on the model by Marchena and Echebarria.[23,24] Importantly, the gating of the RyR2 is stochastic and includes modulation by Csq-2 levels and RyR2 phosphorylation at s2808, giving rise to local release events (sparks). The model also includes transversal and axial tubules reported in previous studies[20,25] as well as a heterogeneous distribution of the number of RyR2s per cluster reported previously.[26] Because of the high resolution of our model (see the Supplemental Mathematical Model for details), we were able to characterize spatio-temporal properties of local calcium release events corresponding to those observed in patients with and without AF (see Supplemental Mathematical Model and Videos 1 and 2). Codes for the mathematical model are available online.[27]

DATA ANALYSIS AND STATISTICAL METHODS. Electrophysiological and molecular biological analysis was performed without knowledge about clinical data, and clinicians had no access to the experimental results. Data were analyzed using IBM SPSS Statistics for Windows (version 26.0). Unless otherwise stated, values were averaged for each patient, and results are expressed as mean ± SEM. Data sets that did not have a normal distribution were represented in box plots with median and 25th and 75th percentiles. Statistical significance was evaluated using chi-square test for categorical data. For normally distributed data (normality was evaluated using Shapiro-Wilk's test and Q-Q plot), the Student's *t*-test was used for paired or unpaired comparisons. For data that did not have a normal distribution, the Wilcoxon rank-sum test was used. Two-way analysis of variance was used for analysis of the impact of AF and the distance to the membrane on Csq-2 and RyR2 distribution and phosphorylation, or the impact of AF and stimulation frequency on the incidence of I_{TI}s or afterdepolarizations, as indicated in text or figure legends. Bonferroni post-hoc test was done for pairwise comparison of differences between groups. A value of $P < 0.05$ was considered statistically significant as indicated in the figures.

RESULTS

PROPERTIES, FREQUENCY, AND DISTRIBUTION OF CALCIUM SPARKS IN PATIENTS WITH AF. Calcium sparks were measured in 146 human atrial myocytes from 79 patients. Of these, 2,971 sparks were detected in 32 patients with AF and 371 sparks were detected in 47 patients without AF. Division of the myocytes in 1-μm wide concentric layers revealed that the spark density in patients with AF was highest at the sarcolemma and declined toward the cell center (**Figures 1A and 1B**). In patients without AF, the spark density increased toward the cell center (**Figure 1B**). Consequently, the spark density was 40-fold higher at the sarcolemma in patients with AF. The same was true for the spark site density (**Figure 1C**). In relative terms, sparks observed within 2 μm from the cell membrane accounted for 63% in patients with AF and 17% in patients without AF ($P = 0.005$). By contrast, sparks occurring at the cell center (4-6 μm from the sarcolemma) accounted for 9% and 46% in patients with and without AF, respectively ($P < 0.001$) (**Figure 1D**, left). Fitting the cumulative incidence of calcium sparks as a function of the distance from the membrane (**Figure 1D**, right) revealed that 50% of the sparks were located within 1 and 4.4 μm from the sarcolemma in patients with and without AF, respectively ($P < 0.001$). The spatial spark distribution was similar in patients with paroxysmal and longstanding persistent or permanent AF (Supplemental Figure 2). Moreover, analysis of the influence of sex showed that although the spark density was higher in women, sex did not affect the spark distribution (Supplemental Figure 3). Furthermore, calcium sparks located at the sarcolemma (SL) displayed a significantly shorter distance to the nearest neighbor in patients with than without AF (2.6 ± 0.5 μm vs 9.5 ± 1.3 μm; $P < 0.001$). This difference was attenuated and nonsignificant for the sparks located at the cell center (2.8 ± 0.4 μm vs 4.2 ± 0.6 μm). Similarly, analysis of the spark properties showed that those located at the SL were smaller, were wider, and decayed more slowly in patients with than without AF (**Figure 2A**) and that these differences were attenuated or abolished for sparks located

FIGURE 1 AF Is Associated With a Preferential Increase in Ca^{2+} Sparks Near the Sarcolemma

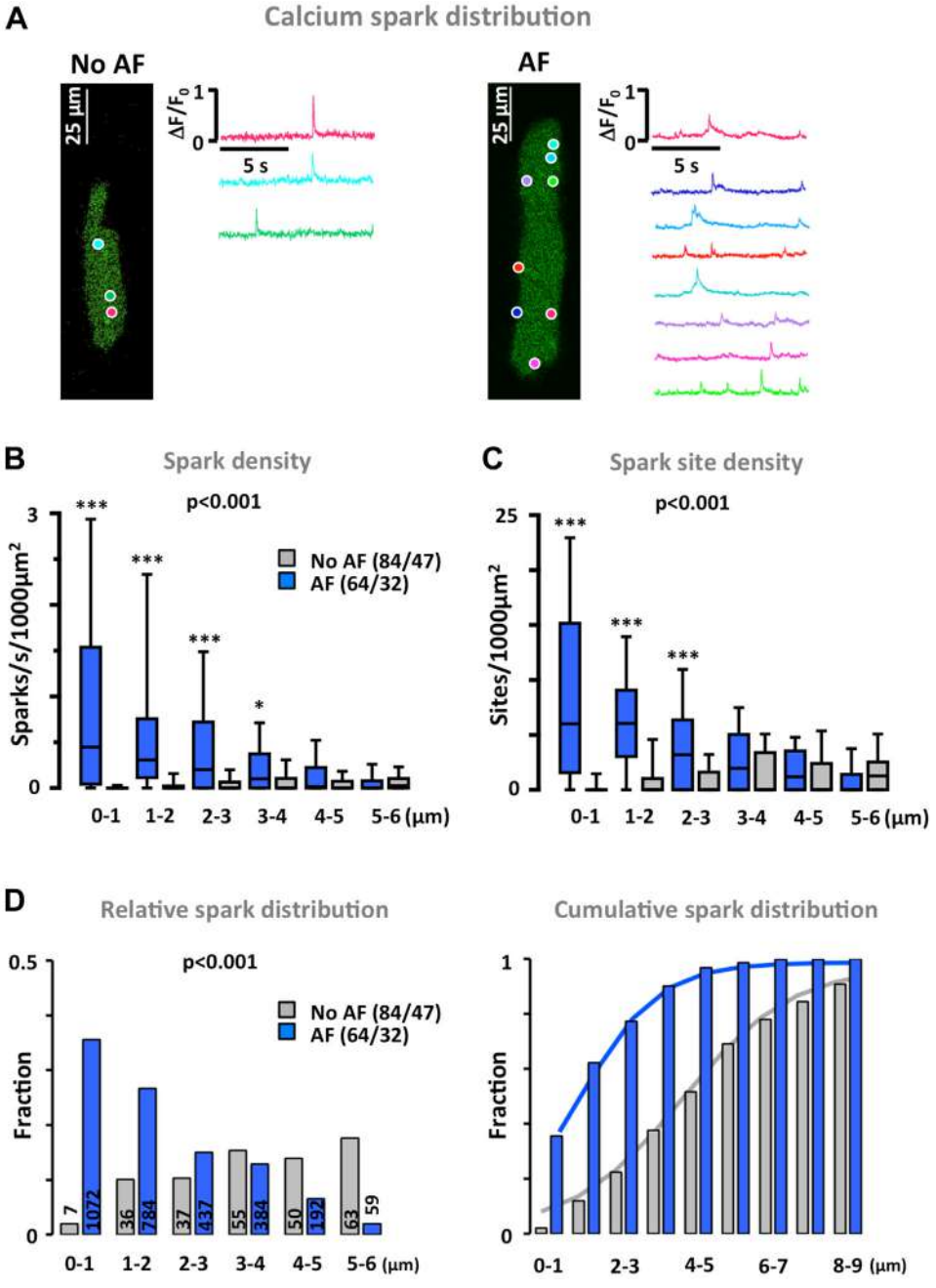

(A) Cardiomyocytes from patients without and with atrial fibrillation (AF). Spark sites are indicated with **circles** and corresponding calcium traces are shown in the same color. Notice the abundant and peripheral spark distribution in AF. **(B)** Spark density as a function of the distance to the sarcolemma. **(C)** Spark site density. Data are given as median ± 25th percentiles. **(D)** Relative **(left)** and cumulative distribution **(right)** of all sparks (numbers of sparks detected are given within each **bar**) in patients without and with AF. Distance to sarcolemma is given **below the bars**. Fitting cumulative distributions with sigmoidal equations are indicated with **solid lines**. Significant differences in the distributions for patients without (no AF) and with AF are indicated with *P* values **above the bars** (Wilcoxon rank-sum test). The number of cells/patients are given in parentheses next to the color codes. Differences between individual pairs are indicated as follows: $*P < 0.05$; $***P < 0.001$.

FIGURE 2 Impact of AF on Calcium Sparks Near the Sarcolemma and the Cell Center

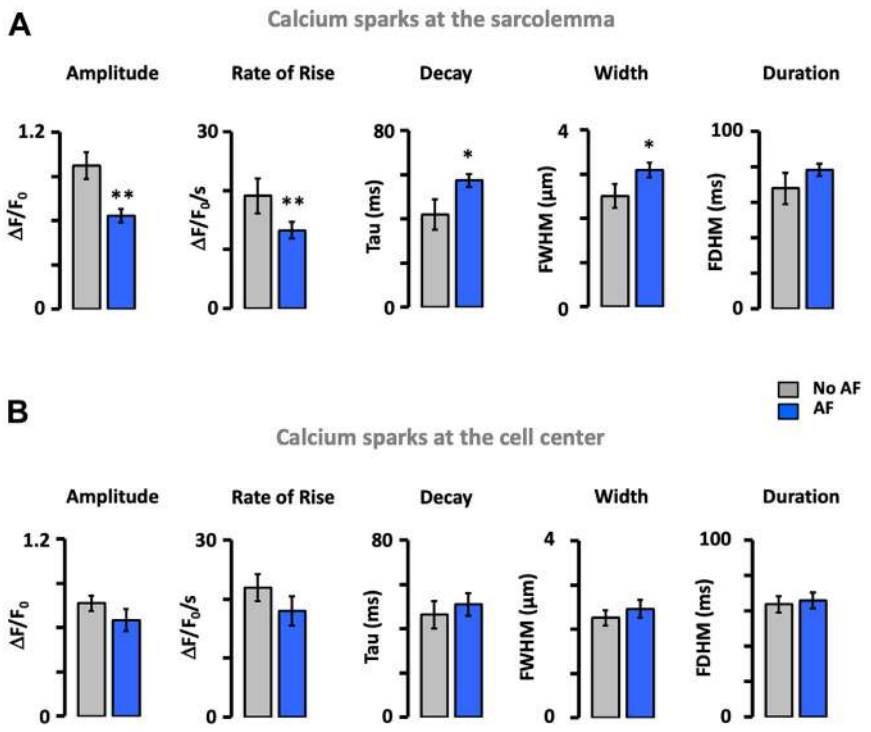

(A) Calcium spark amplitude, rate of rise, decay constant, full width at half maximum, and full duration at half maximum were measured at the sarcolemma (0-2 μm from the sarcolemma) in 35 myocytes from 28 patients without (no atrial fibrillation [AF]) and 51 myocytes from 28 patients with AF. **(B)** The same parameters were measured in the cell center (3-7 μm from the sarcolemma) of the same myocytes as in **A**. Data are given as mean ± SEM. Significant differences between patients without and with AF are indicated as follows: $*P < 0.05$; $**P < 0.01$ (Student's *t*-test).

in the cell center (**Figure 2B**). This, combined with the higher frequency and smaller distance between sparks at the SL in patients with AF, is expected to facilitate the fusion of neighboring sparks into calcium waves or transients near the sarcolemma.

MECHANISMS UNDERLYING CHANGES IN CALCIUM SPARK DISTRIBUTION AND DYNAMICS IN AF. To identify molecular mechanisms underlying a higher spark density at the sarcolemma, we first measured the caffeine releasable SR calcium content, which has been proposed to regulate spontaneous calcium release from the SR. However, the caffeine-sensitive SR calcium load was significantly smaller in patients with AF (Supplemental Figures 4A and 4B). In line with this, the expression of SERCA2a, which regulates SR calcium loading, was smaller in patients with AF (Supplemental Figure 4C). Moreover, the ratios SERCA2a/PLB, PLBs16/PLB, and PLBt17/PLB, which determine the SERCA2a activity, were similar in patients with and without AF (Supplemental Figures 4D and 4F). Similarly, analysis of the NCX-1 rate as a function of the calcium available for extrusion showed no difference between patients with and without AF (Supplemental Figures 4G and 4H), a notion that is supported by unchanged NCX-1 expression in AF (Supplemental Figure 4I). Together, these results indicate that the higher spark density at the sarcolemma observed in patients with AF is neither caused by a higher SR calcium load nor by a lower NCX-1 activity.

We then performed immunofluorescent labeling of the RyR2 clusters that give rise to calcium sparks and of the Cav1.2 that trigger calcium release through the RyR2s during excitation-contraction coupling. **Figure 3** shows that although both the RyR2 (**Figures 3A and 3B**) and Cav1.2 densities (**Figures 3C and 3E**) were higher at the SL, there was no difference in RyR2 (**Figure 3B**) or the Cav1.2 distribution (**Figure 3E**) among patients with and without AF.

On the other hand, ratiometric immunofluorescent analysis of s2808 phosphorylated RyR2 (**Figures 4A**

FIGURE 3 **Effect of AF on the Spatial RyR2 and L-type Calcium Channel Distribution**

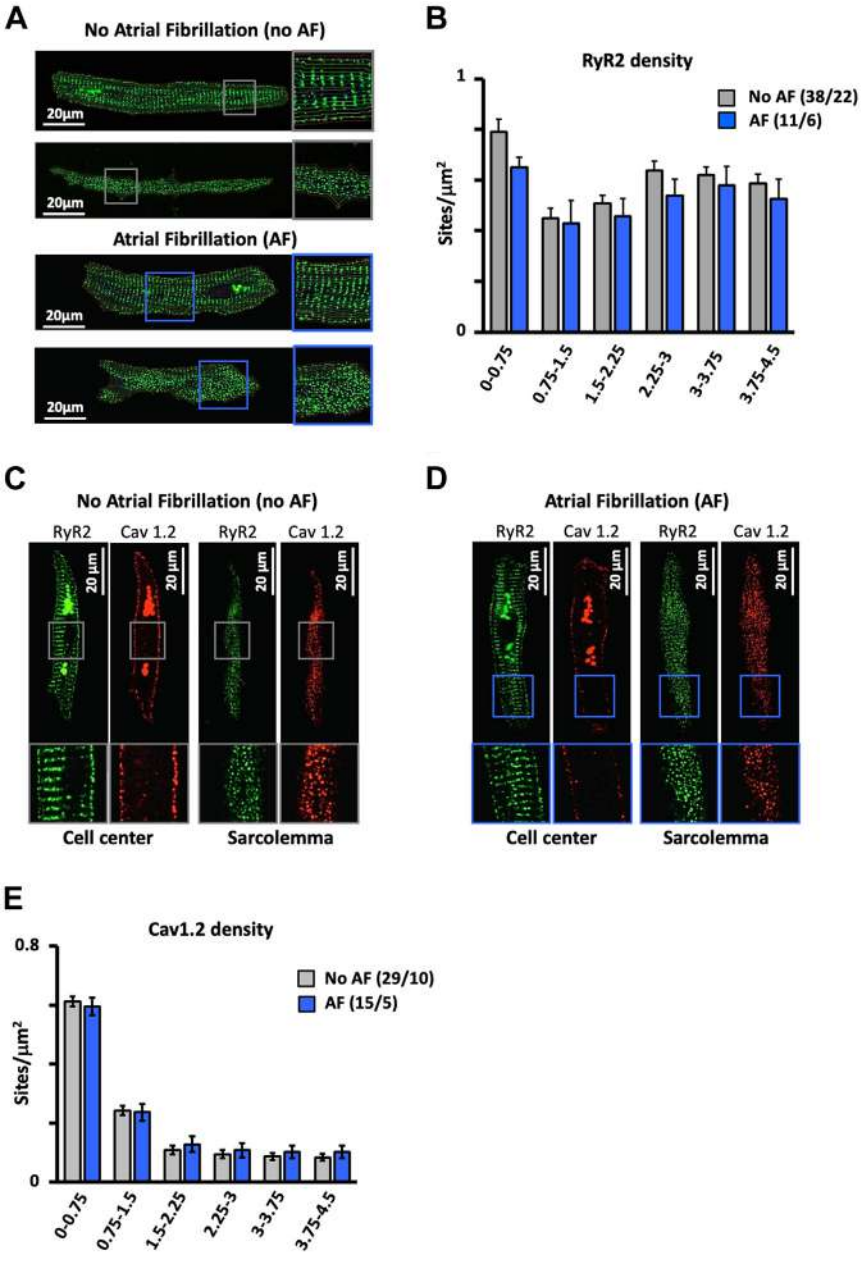

(A) RyR2 distribution in the cell center and at the sarcolemma in atrial myocytes from patients without and with atrial fibrillation (AF). **(B)** RyR2 density as a function of the distance to the sarcolemma (given below **bars** in μm) in patients with no AF and with AF. **(C and D)** Spatial RyR2 distribution **(green)** and L-type calcium channel (Cav1.2) distribution **(red)** at the cell center and the sarcolemma in myocytes from a patient with no AF **(C)** and one with AF **(D)**. **(E)** Cav1.2 density as a function of the distance to the sarcolemma (given **below bars** in μm) in patients with no AF and with AF. Data are given as mean ± SEM. The number of myocytes/patients is given in **parentheses**.

and 4B, Supplemental Figure 5) showed that s2808 phosphorylation was 75% higher in myocytes from patients with than without AF, and highest near the sarcolemma ($P < 0.001$). By contrast, phosphorylation at s2814 was low throughout myocytes and was not different between patients with and without AF (**Figures 4C and 4D**, Supplemental Figure 6). Labeling of RyR2 and Csq-2 revealed a higher Csq-2 density (Csq-2/RyR2 ratio) at the sarcolemma than the cell center ($P < 0.001$) in patients with and without AF

FIGURE 4 AF Increases RyR Phosphorylation and Decreases Csq-2 at the Sarcolemma

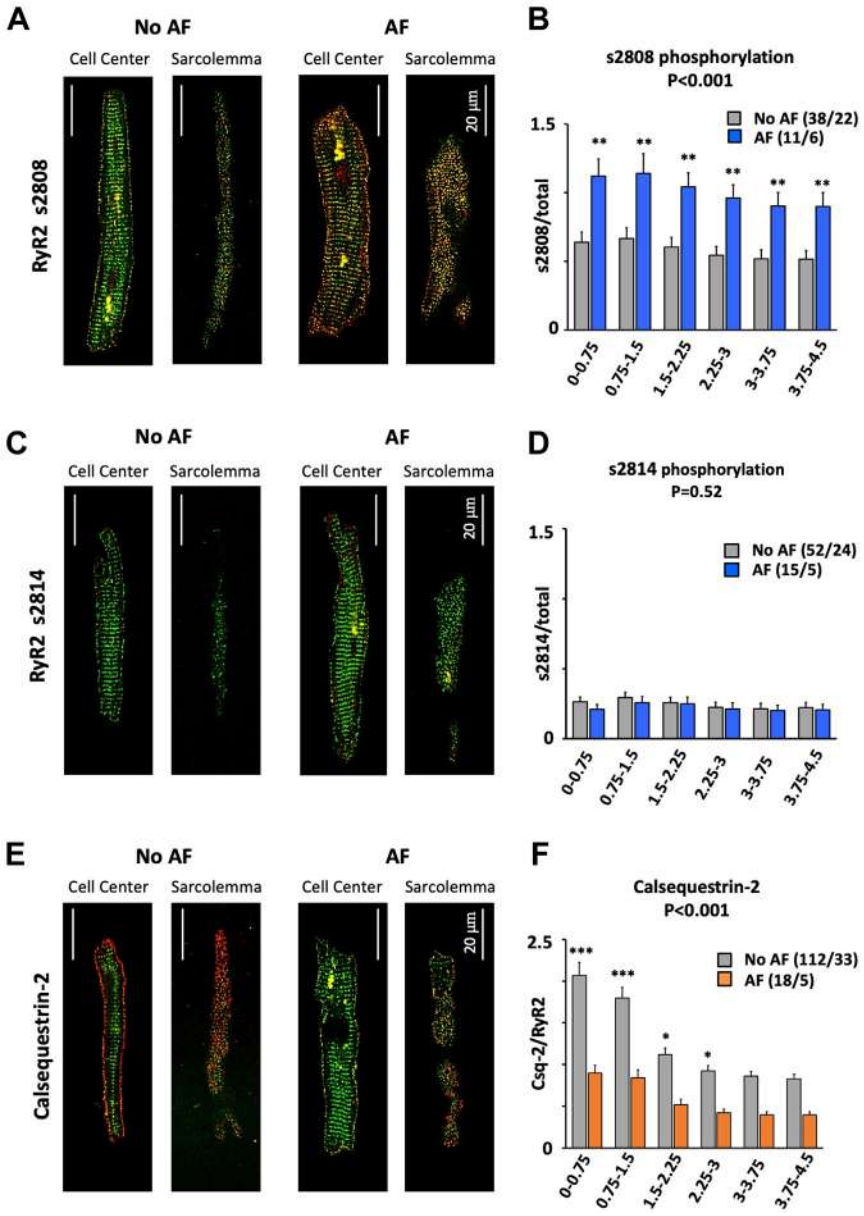

(A) Total RyR2 **(green)** and s2808 phosphorylated RyR2 **(red)** in patients without and with atrial fibrillation (AF). **(B)** S2808 phosphorylation (s2808/total RyR2) vs distance to the sarcolemma. **(C)** Total RyR2 **(green)** and s2814 phosphorylated RyR2 **(red). (D)** S2814 phosphorylation (s2814/total RyR2) vs distance to sarcolemma. **(E)** Total RyR2 **(green)** and Csq-2 **(red). (F)** Csq-2/total RyR2 ratio vs distance to the sarcolemma. Data are given as mean ± SEM. The number of myocytes/patients is indicated in **parenthesis**. The *P* values **above the graphs** indicate significant differences between patients without (no AF) and with AF (2-way analysis of variance). Asterisks indicate a significant difference between AF and no AF for each cell segment (Bonferroni post hoc test). *$P < 0.05$; **$P < 0.01$; ***$P < 0.001$.

(**Figures 4E and 4F**, Supplemental Figure 7). Moreover, the Csq-2 density was significantly lower in patients with than without AF ($P < 0.001$) throughout the myocyte (**Figure 4F**).

Together, these findings suggest that changes in RyR2 phosphorylation and Csq-2 expression underlie the preferential distribution of calcium sparks at the sarcolemma in AF. To study how the observed

alterations in Csq-2 expression and s2808 phosphorylation affect RyR2 activity, we modified a mathematical human atrial myocyte model[24] with a high spatial resolution (100 nm), including modulation of RyR2 gating by Csq-2 and RyR2 phosphorylation. The model also included axial/t-tubular structures that were considered proportional to the Cav1.2 distribution shown in **Figure 3E**. **Figure 5A** shows the RyR2 distribution, the spark heat map, and the spatial event distribution at baseline. The model incorporated data from **Figure 4** to modulate RyR2 opening by the Csq-2 level at each RyR2 cluster (**Figure 5B**) and by the RyR2 phosphorylation at s2808 (**Figure 5C**). As shown in **Figure 5D**, modulation of the RyR2 activity by the Csq-2 level resulted in a higher spark density at the cell center in patients without AF and a fairly uniform event distribution in patients with AF. When modulation of RyR2 activity by s2808 phosphorylation was included in the mathematical model, sparks were most frequent at the sarcolemma in patients with and without AF (**Figure 5E**). However, when combining the effects of Csq-2 and s2808 phosphorylation on RyR2 activity, the model yielded calcium sparks (see Videos 1 and 2) with spatial distributions and relative densities (**Figure 5F**) that were very similar to those observed in atrial myocytes from patients without and with AF (compare to **Figure 1D**).

FUNCTIONAL CONSEQUENCES OF SUBSARCOLEMMAL CALCIUM RELEASE IN PATIENTS WITH AF. Comparative analysis of individual calcium waves and the resulting I_{TI} currents showed that even though there were no significant differences in the amplitude of the calcium transient among patients with and without AF, the amplitude of the resulting I_{TI} was significantly higher in those with AF (**Figures 6A and 6B**). Consequently, the ratio of the I_{TI} and calcium wave amplitude was twice as high in AF (1.63 ± 0.33 vs 0.75 ± 0.12; $P = 0.010$). Moreover, the higher I_{TI} amplitude (0.51 ± 0.08 vs 0.27 ± 0.05; $P = 0.029$) and I_{TI} frequency (2.1 ± 0.4 vs 0.46 ± 0.10; $P < 0.001$) in AF was associated with higher amplitude (11.25 ± 1.72 vs 6.92 ± 1.31; $P = 0.019$) and incidence (3.36 ± 0.68 vs 1.45 ± 0.68; $P = 0.010$) of afterdepolarizations in myocytes from the same patients (**Figure 6C**). This is summarized in **Figure 6D** and supports the notion that calcium release-induced I_{TI}s elicit spontaneous membrane depolarizations.

On the other hand, 50 nmol/L nifedipine reduced the I_{Ca} density in patients without AF (from 2.0 ± 0.3 to 1.3 ± 0.2 pA/pF; $P = 0.004$; n = 10) to levels observed in patients with AF, but it did not affect the I_{TI} frequency in the same patients (0.78 ± 0.27 events/min vs 0.78 ± 0.26 events/min). This suggests that the L-type calcium channel plays a minor role in regulating the I_{TI} frequency at rest and that it is unlikely to cause a higher incidence of I_{TI}s observed in patients with AF.

Finally, to facilitate translation, we tested if the previously mentioned spontaneous calcium release-induced electrical activity observed in resting myocytes occur in beating myocytes as well. As shown in **Figures 7A and 7B**, the fraction of myocytes presenting spontaneous I_{TI}s during electrical stimulation increased at higher pacing frequencies ($P < 0.001$), and this phenomenon was exacerbated in AF ($P = 0.003$). Likewise, myocytes from patients with AF subjected to the current-clamp technique showed a strong increase in the fraction of spontaneous early or delayed afterdepolarizations during the pacing protocol ($P < 0.001$) (**Figures 7C and 7D**).

DISCUSSION

MAIN FINDINGS. The present study is the first to analyze the spatio-temporal distribution of calcium sparks in human atrial myocytes and show that AF is associated with a preferential distribution of sparks at the sarcolemma. Moreover, we show that the differential increase in SR calcium release near the sarcolemma increases the fraction of calcium extruded by electrogenic NCX, affording a mechanistic explanation for the larger and more frequent afterdepolarizations observed in myocytes from patients with AF. This phenomenon was not caused by alterations in I_{Ca} density or NCX-1 activity, nor was it caused by changes in the distribution of Cav1.2 or RyR2. Instead, immunofluorescent labeling and mathematical modeling showed that a differential increase in the spark density near the SL can be accounted for by the observed changes in the distribution of Csq-2 and s2808-phosphorylated RyR2 in patients with AF. Together, these findings highlight local membrane-specific up-regulation of RyR2 activity in AF and point to G-protein coupled membrane receptors that modulate cAMP metabolism as specific targets to prevent excessive RyR2 phosphorylation at the sarcolemma, dissipate the spontaneous calcium release gradient, and attenuate or abolish afterdepolarizations in AF.

INFLUENCE OF CALCIUM REGULATORY PROTEINS ON THE SPATIAL DISTRIBUTION OF CALCIUM SPARKS IN HUMAN ATRIAL MYOCYTES. We here demonstrate that differences in the spatial distribution of Csq-2 levels and RyR2 phosphorylation at s2808 between patients with and without AF could explain the differences in the distribution and incidence of sparks in atrial myocytes from these patients. Importantly, the findings also suggest that

FIGURE 5 RyR2 Phosphorylation at s2808 and the Csq-2 Level Determine the Spark Distribution in Patients With and Without AF

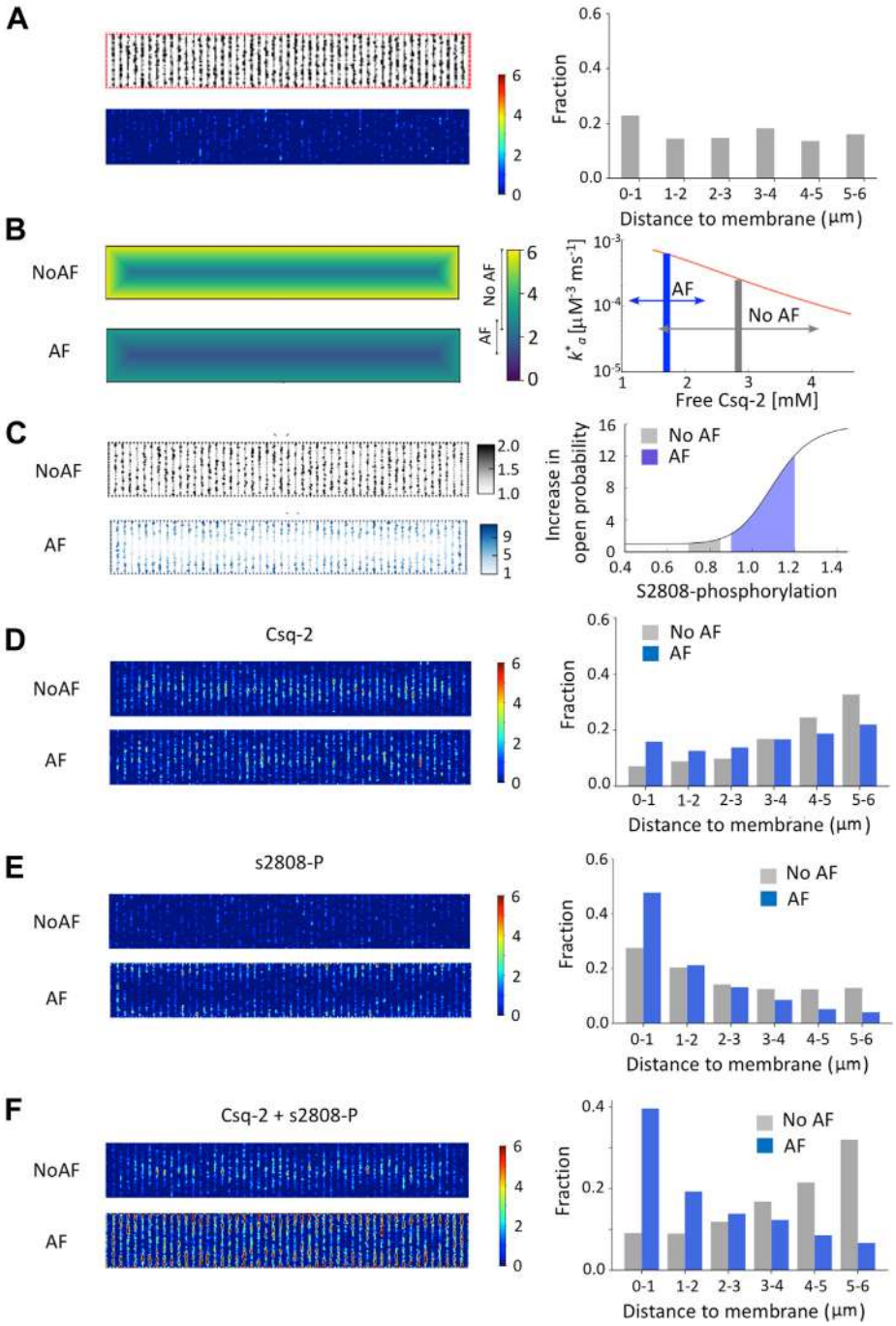

(A) RyR2 distribution in a myocyte model was used to simulate the effects of Csq-2 and s2808 phosphorylation on spark activity. The resulting heat map at baseline is shown **below** and the spatial event distribution is shown on the **right**. **(B)** The effect of Csq-2 level and distribution **(left)** on RyR2 activity **(right).** The effective RyR open probability depends on the amount of free Csq-2, with a range that differs for atrial fibrillation (AF) **(blue arrow)** and NoAF **(gray arrow). (C)** Distribution of s2808 phosphorylated RyR2 in the model **(left)** and its effect on RyR2 activity **(right).** RyR2 open probability is assumed to depend on phosphorylation at s2808 in a sigmoidal fashion. **Gray and blue areas** correspond to the ranges for s2808 phosphorylation in NoAF and AF (from Figure 4B). **(D to F)** Spark heat maps **(left)** and spatial event distribution **(right)** are shown, taking into account Csq-2 levels and distribution **(D),** s2808 level and distribution **(E),** and the combined effects of Csq-2 and s2808 phosphorylation **(F).**

FIGURE 6 **AF Increases the Amplitude and Incidence of Ca^{2+} Release-Induced I_{TI}s**

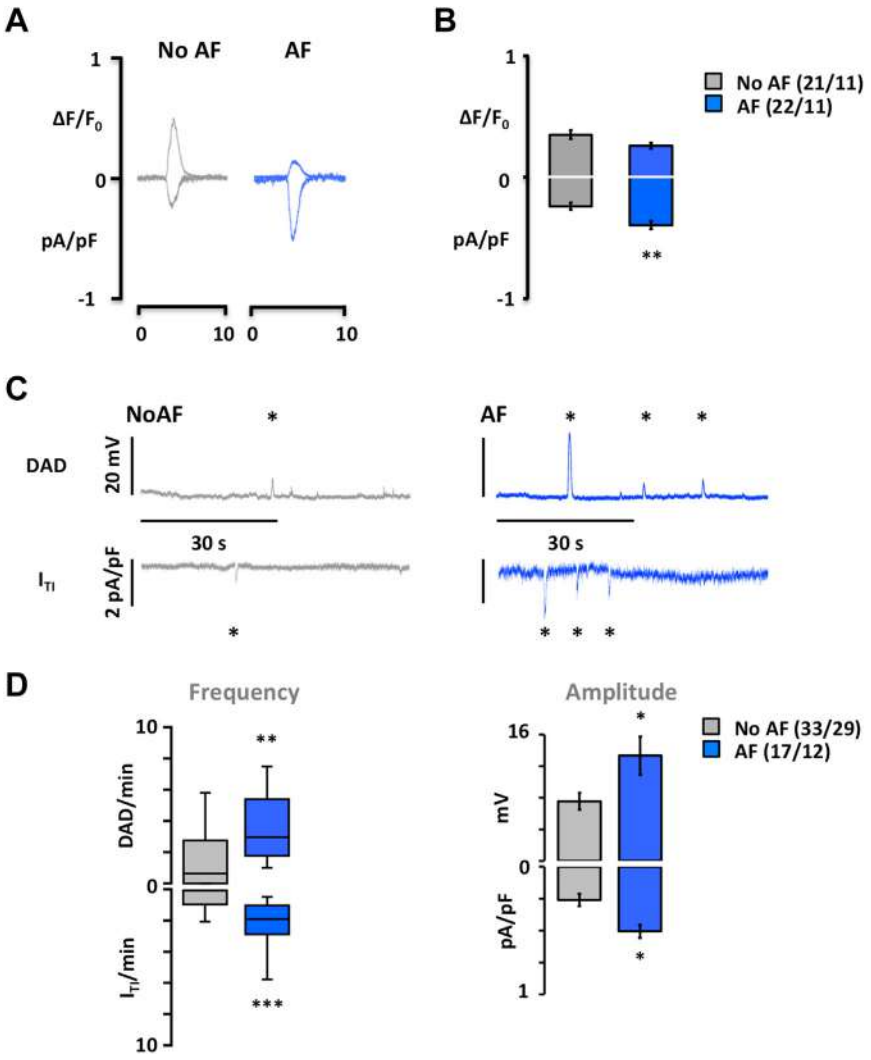

(A) Calcium wave recordings ($\Delta F/F_O$) and the resulting I_{TI} currents from patients without (No atrial fibrillation [AF]) and with AF. **(B)** Ca^{2+} wave amplitude and I_{TI} current density. Notice that for similar calcium transients, the resulting I_{TI} amplitude is larger in AF. **(C)** Consecutive recordings of spontaneous membrane depolarization (DAD) and I_{TI}. **(D)** Frequency and amplitude of DADs and I_{TI}s. Data are given as mean ± SEM or median ± 25 percentiles (frequency, **D**). The number of myocytes/patients is indicated in **parenthesis** and statistical significance for comparisons (Wilcoxon rank-sum [frequency, **D**] or Student's *t*-test [**B** and amplitude **D**]) are **given above and below bars**. *$P < 0.05$; **$P < 0.01$; ***$P < 0.001$.

pathological alterations in the expression or activity of membrane receptors regulating RyR2 phosphorylation could explain why phosphorylation persists in isolated myocytes and be a trigger for the observed redistribution and higher incidence of calcium sparks near the sarcolemma in AF. In this regard, a higher incidence of sparks in AF has previously been associated with increased expression and activation of Gs protein-coupled adenosine A_{2A} receptors by endogenous adenosine,[14] and we have recently shown that a higher I_{TI} frequency in patients with AF was abolished in those treated with adenosine deaminase or beta-adrenergic receptor blockers.[19] AF has also been associated with increased RyR2 phosphorylation at s2814,[12,13,28] but we here found that RyR2 phosphorylation at s2814 phosphorylation was uniform and low both in patients with and without AF.

FIGURE 7 AF Potentiates Spontaneous Electrical Activity in Human Atrial Myocytes

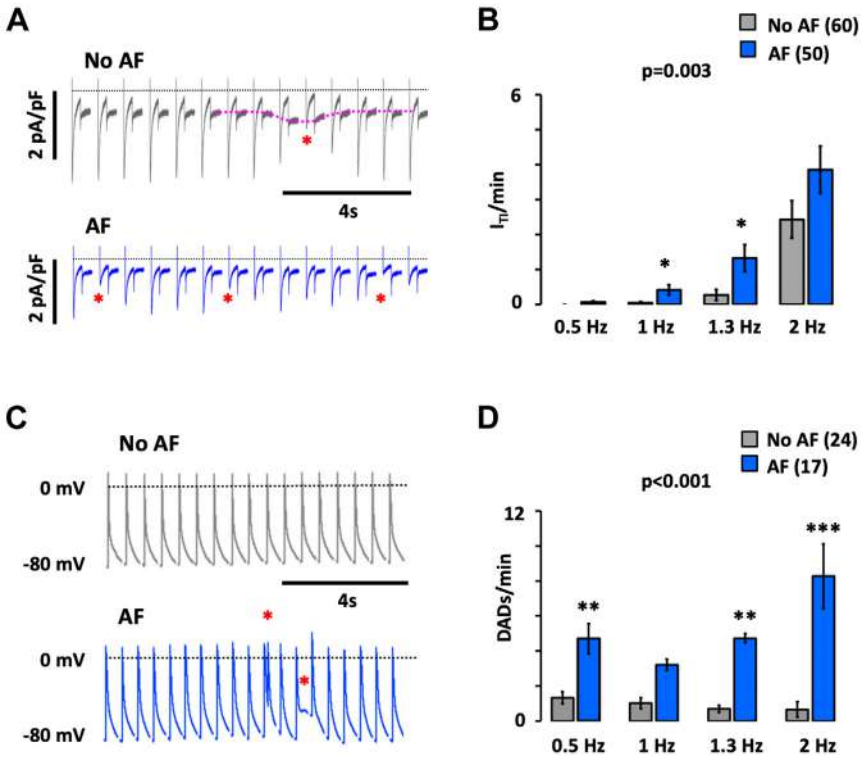

(A) Current recordings in myocytes from patients without and with AF. A spontaneous I_{TI} current is indicated with a **dotted red line,** and the resulting reduction in I_{Ca} density is indicated with an **asterisk**. **(B)** Incidence of spontaneous I_{TI}s at increasing stimulation frequencies (given **below bars**). **(C)** Action potential recordings in myocytes from patients without and with AF. Spontaneous membrane depolarizations are indicated with an **asterisk**. **(D)** Incidence of spontaneous depolarizations at increasing stimulation frequencies (given **below bars**). Data are given as mean ± SEM. The number of patients is indicated in **parenthesis**. The *P* values **above graphs** indicate the statistical differences between patients without (no AF) and with AF (2-way analysis of variance). **Asterisks** indicate a statistically significant difference between AF and no AF for each frequency (Bonferroni post hoc test). **P* < 0.05; ***P* < 0.01; ****P* < 0.001.

Theoretically, a higher spark density at the sarcolemma could also result from a lower NCX-1 activity, assuming that t-tubular structures are scarce in human right atrial myocytes as suggested by previous reports.[10,21,25] However, no previous studies have reported decreased NCX-1 expression in AF, whereas some have reported higher NCX-1 expression and activity in AF.[7,11] The latter would be expected to lower calcium near the sarcolemma and diminish RyR2 activation, which is difficult to reconcile with the higher spark frequency observed at the sarcolemma in myocytes from patients with AF. Here, we found no evidence of changes in the NCX-1 rate or expression, nor did we find changes in the expression of proteins regulating SR calcium uptake or SR calcium load. This is in line with previous reports finding similar or decreased SERCA2a expression[29,30] or SERCA2a/PLB ratios in AF,[11] discarding NCX-1, SERCA2a, or PLB as mediators of the observed changes in calcium spark distribution in patients with AF. Furthermore, a recent study analyzing the calcium signal in individual GFP-tagged RyR2 clusters showed that the spark frequency determines the SR calcium load. Thus, clusters with the highest incidence of sparks displayed the lowest SR calcium load, whereas RyR2 clusters without any sparks had the highest SR calcium load.[31] Together, these results strongly suggest that a differential increase in RyR2 phosphorylation near the sarcolemma underlies the higher incidence of sparks at this location in patients with AF.

Finally, a higher spark frequency near the sarcolemma has been observed and attributed to RyR2 activation by L-type calcium channels in cat atrial myocytes.[32] However, we found that partial I_{Ca} inhibition, used to mimic a reduced I_{Ca} density in patients with AF,[10,33,34] did not affect the spontaneous I_{TI} frequency. This finding was reproduced by

FIGURE 8 **The Mechanism Underlying Spontaneous Ca^{2+} Release Near the Sarcolemma in AF**

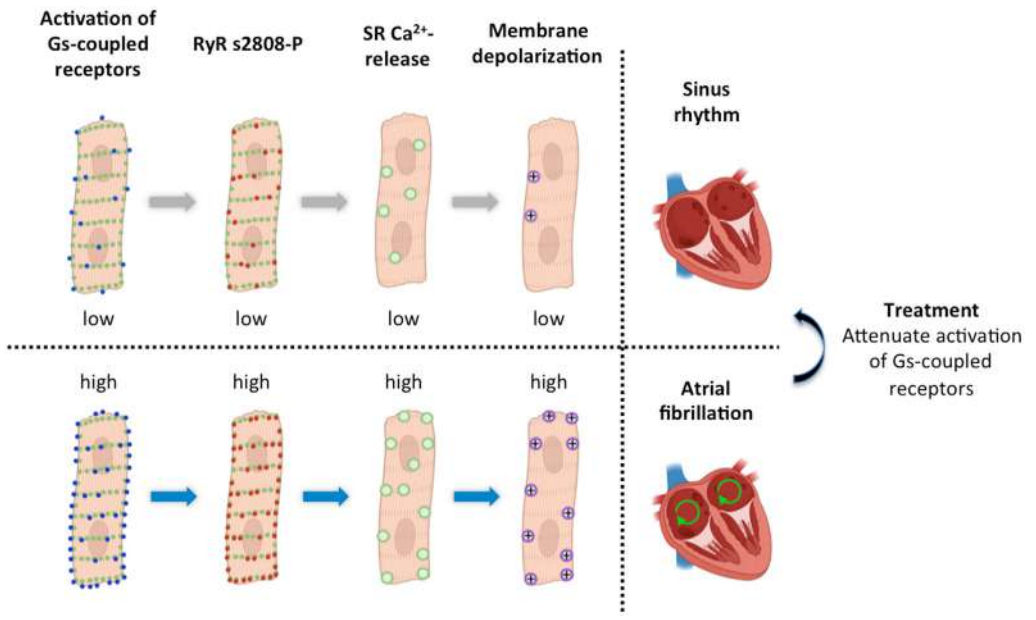

Patients with atrial fibrillation (AF) display preferential RyR2 phosphorylation at s2808 near the sarcolemma. As a result, more RyR2s will reach the threshold for spontaneous calcium release, increasing spontaneous calcium release near the sarcolemma. Consequently, a larger fraction of the released calcium will be extruded by electrogenic Na^{+}-Ca^{2+} exchange giving rise to larger membrane depolarizations. This, in turn, increases the likelihood that these afterdepolarizations induce ectopic activity capable of perturbing the normal atrial rhythm and initiating AF. Together, these findings suggest that Gs-protein coupled membrane receptors that regulate RyR2 phosphorylation at s2808 could be upstream targets to normalize the incidence and distribution of spontaneous calcium release events in AF and prevent the induction of arrhythmogenic afterdepolarizations.

mathematical modeling, suggesting that a prominent RyR2 activation by L-type calcium channels seems an unlikely explanation for the higher spark density near the sarcolemma in patients with AF.

CALCIUM RELEASE AT THE SARCOLEMMA IS KEY TO A HIGHER INCIDENCE AND AMPLITUDE OF AFTERDEPOLARIZATIONS IN AF. The higher density, longer duration, and shorter distance between sparks in patients with AF are expected to facilitate the fusion of sparks and explain a higher incidence of I_{Ti}s in AF.[1,5,35] Here, we demonstrate that preferential distribution of these sparks near the sarcolemma also leads to extrusion of a larger fraction of spontaneously released calcium by the NCX-1, which translates into larger and more frequent afterdepolarizations in AF.

Furthermore, we show that when spontaneous calcium release, I_{TI}, or afterdepolarizations occur at rest, they are also observed upon electrical pacing of the myocytes, leading to irregular beating patterns. Previous studies have suggested that calcium transients propagate from the sarcolemma to the cell center in paced human atrial myocytes[10] with RyR2 clusters in the cell center being activated through calcium-induced calcium release.[32] Therefore, excessive spontaneous calcium release near the sarcolemma in AF would be expected to favor heterogeneous propagation of the calcium transient toward the cell center and facilitate the induction of irregular responses at high pacing rates. This translation of spontaneous electrical activity at rest to irregular beating in paced myocytes provides a mechanistic explanation for previous findings showing that human atrial myocytes with a high intrinsic I_{TI} frequency present a higher incidence of alternating or irregular beat-to-beat responses, especially upon elevation of the pacing rate.[10,36]

STUDY LIMITATIONS. A general limitation with human atrial samples is the potential influence of concurrent disease and pharmacological treatments, and we cannot exclude that an uneven distribution of clinical factors (see Supplemental Table 1) could

affect some of the observed differences between patients with and without AF. Even so, sparks, I_{TI}, and afterdepolarizations are consistently and repeatedly found elevated in patients with AF, suggesting that these observations are robust. On the other hand, we cannot rule out that some findings could be specific to the right atrium.

Opposite to previous studies, we find no evidence of higher RyR2 phosphorylation at s2814 in patients with AF. However, we cannot rule out that this difference is caused by differences in the experimental approach used to determine RyR2 phosphorylation. Thus, the present study uses immunofluorescent labeling of isolated atrial myocytes at rest to visualize the spatial distribution of the RyR2s and s2814 phosphorylated RyR2s. By contrast, previous studies are largely based on the Western blot technique in cardiac tissue samples, and it is possible that the calcium level and consequently s2814 phosphorylation is lower in resting myocytes than in samples used for Western blotting.[28] Similarly, we cannot exclude a role for cAMP-dependent phosphorylation of the RyR2 at s2030 as a modulator of spontaneous calcium release, but we are unable to detect s2030 phosphorylation in human atrial myocytes with currently available antibodies.

Spatial heterogeneities in calcium release from the SR have also been attributed to heterogeneities in axial and t-tubular structures in atrial myocytes.[20] However, previous studies failed to find extensive t-tubular structures in human right atrial myocytes,[21,25] and more importantly, axial tubular structures are primarily located in the cell center and therefore unlikely to account for a high spark density at the sarcolemma.

CONCLUSIONS

This study highlights the crucial importance of the spatio-temporal distribution of spontaneous calcium release events and documents that a differential increase in calcium release near the sarcolemma is key to increased amplitude and incidence of afterdepolarizations in atrial myocytes from patients with AF. The findings are summarized schematically in **Figure 8**, highlighting the RyR2 phosphorylation at s2808 as a modulator of local calcium release events. In particular, our findings afford a physiological basis for testing Gs-protein coupled receptors that modulate cAMP-dependent RyR2 phosphorylation[14,19] as upstream targets for pharmacological control of spontaneous electrical activity in patients with AF through regulation of spontaneous calcium release near the sarcolemma.

ACKNOWLEDGMENTS The authors greatly appreciate the collaboration of the Cardiac Surgery Team at Hospital de la Santa Creu i Sant Pau.

FUNDING SUPPORT AND AUTHOR DISCLOSURES

This work was supported by grants from the Spanish Ministry of Science and Innovation and Universities (SAF2017-88019-C3-1-R and PID2020-116927RB-C21 to Dr Hove-Madsen, SAF2017-88019-C3-3-R to Dr Benítez, SAF2017-88019-C3-2-R to Dr Echebarria; and PID2020-116927RB-C22 to Dr Benítez and Dr Echebarria); from the Spanish Ministry of Health, Consume and Social Welfare, CIBERCV (CB16/11/00276 to Dr Cinca); from Generalitat de Catalunya (SGR2017-1769 to Dr Hove-Madsen and PERIS SALUT-16 to Dr Llach); a grant from the Spanish Society of Cardiology (to Dr Hove-Madsen); and grants from Fundació Marató TV3 (Marato2015-20-30 to Dr Hove-Madsen, Marato2015-20-31 to Dr Ciruela, and Marato2015-11-10 to Dr Echebarria). All other authors have reported that they have no relationships relevant to the contents of this paper to disclose.

ADDRESS FOR CORRESPONDENCE: Dr Leif Hove-Madsen, Cardiac Rhythm and Contraction Group, Biomedical Research Institute Barcelona, Hospital de la Santa Creu i Sant Pau, St Antoni Mª Claret 167, 08025 Barcelona, Spain. E-mail: leif.hove@iibb.csic.es.

PERSPECTIVES

COMPETENCY IN MEDICAL KNOWLEDGE: Spontaneous calcium release events favor the induction of afterdepolarizations in patients with AF, but the importance of their spatial subcellular distribution is unknown. We showed that the spatial distribution of local calcium release events (sparks) determines their ability to induce afterdepolarizations in human atrial myocytes, and that a 40-fold higher incidence of calcium sparks near the sarcolemma in patients with AF is key to the higher incidence of afterdepolarizations in these patients.

TRANSLATIONAL OUTLOOK: Our data identified RyR2 phosphorylation at s2808 as a key mechanism associated with a differential increase in calcium release near the sarcolemma and points to mechanisms that regulate RyR2 phosphorylation at the sarcolemma, such as G-protein coupled membrane receptors, as upstream therapeutic targets for selective attenuation of spontaneous calcium release near the sarcolemma. Further studies testing the efficacy of Gs-protein coupled receptor blockers in reducing spontaneous electrical activity are necessary to ascertain if the findings can be translated to the treatment of patients with ectopic atrial activity or AF.

REFERENCES

1. Hove-Madsen L, Llach A, Bayes-Genis A, et al. Atrial fibrillation is associated with increased spontaneous calcium release from the sarcoplasmic reticulum in human atrial myocytes. *Circulation*. 2004;110(11):1358–1363.

2. Lai LP, Su MJ, Lin JL, et al. Down-regulation of L-type calcium channel and sarcoplasmic reticular Ca(2+)-ATPase mRNA in human atrial fibrillation without significant change in the mRNA of ryanodine receptor, calsequestrin and phospholamban: an insight into the mechanism of atrial electrical remodeling. *J Am Coll Cardiol*. 1999;33(5):1231–1237.

3. Van Wagoner DR, Pond AL, Lamorgese M, Rossie SS, McCarthy PM, Nerbonne JM. Atrial L-type Ca2+ currents and human atrial fibrillation. *Circ Res*. 1999;85(5):428–436.

4. Vest JA, Wehrens XH, Reiken SR, et al. Defective cardiac ryanodine receptor regulation during atrial fibrillation. *Circulation*. 2005;111(16):2025–2032.

5. Voigt N, Li N, Wang Q, et al. Enhanced sarcoplasmic reticulum Ca2+ leak and increased Na+-Ca2+ exchanger function underlie delayed afterdepolarizations in patients with chronic atrial fibrillation. *Circulation*. 2012;125(17):2059–2070.

6. Voigt N, Heijman J, Wang Q, et al. Cellular and molecular mechanisms of atrial arrhythmogenesis in patients with paroxysmal atrial fibrillation. *Circulation*. 2014;129(2):145–156.

7. Dobrev D, Voigt N, Wehrens XHT. The ryanodine receptor channel as a molecular motif in atrial fibrillation: pathophysiological and therapeutic implications. *Cardiovasc Res*. 2011;89(4):734–743.

8. Nattel S. New ideas about atrial fibrillation 50 years on. *Nature*. 2002;415(6868):219–226.

9. Wakili R, Voigt N, Kaab S, Dobrev D, Nattel S. Recent advances in the molecular pathophysiology of atrial fibrillation. *J Clin Invest*. 2011;121(8):2955–2968.

10. Llach A, Molina CE, Fernandes J, Padró J, Cinca J, Hove-Madsen L. Sarcoplasmic reticulum and L-type Ca $^{2+}$ channel activity regulate the beat-to-beat stability of calcium handling in human atrial myocytes. *J Physiol*. 2011;589(13):3247–3262.

11. El-Armouche A, Boknik P, Eschenhagen T, et al. Molecular determinants of altered Ca2+ handling in human chronic atrial fibrillation. *Circulation*. 2006;114(7):670–680.

12. Greiser M, Neuberger HR, Harks E, et al. Distinct contractile and molecular differences between two goat models of atrial dysfunction: AV block-induced atrial dilatation and atrial fibrillation. *J Mol Cell Cardiol*. 2009;46(3):385–394.

13. Neef S, Maier LS. Remodeling of excitation-contraction coupling in the heart: inhibition of sarcoplasmic reticulum Ca(2+) leak as a novel therapeutic approach. *Curr Hear Fail Rep*. 2007;4(1):11–17.

14. Llach A, Molina CE, Prat-Vidal C, et al. Abnormal calcium handling in atrial fibrillation is linked to up-regulation of adenosine A2A receptors. *Eur Hear J*. 2011;32(6):721–729.

15. Bai Y, Jones PP, Guo J, et al. Phospholamban knockout breaks arrhythmogenic Ca2+ waves and suppresses catecholaminergic polymorphic ventricular tachycardia in mice. *Circ Res*. 2013;113(5):517–526.

16. Herraiz-Martínez A, Llach A, Tarifa C, et al. The 4q25 variant rs13143308T links risk of atrial fibrillation to defective calcium homoeostasis. *Cardiovasc Res*. 2019;115(3):578–589.

17. Neef S, Dybkova N, Sossalla S, et al. CaMKII-dependent diastolic SR Ca2+ leak and elevated diastolic Ca2+ levels in right atrial myocardium of patients with atrial fibrillation. *Circ Res*. 2010;106(6):1134–1144.

18. Díaz ME, Trafford AW, O'Neill SC, Eisner DA. A measurable reduction of s.r. Ca content follows spontaneous Ca release in rat ventricular myocytes. *Pflügers Arch Eur J Physiol*. 1997;434(6):3. https://doi.org/10.1007/s004240050475

19. Herraiz-Martínez A, Tarifa C, Jiménez-Sábado V, et al. Influence of sex on intracellular calcium homeostasis in patients with atrial fibrillation. *Cardiovasc Res*. 2022;118(4):1033–1045.

20. Brandenburg S, Kohl T, Williams GSB, et al. Axial tubule junctions control rapid calcium signaling in atria. *J Clin Invest*. 2016;126(10):3999–4015.

21. Herraiz-Martínez A, Álvarez-García J, Llach A, et al. Ageing is associated with deterioration of calcium homeostasis in isolated human right atrial myocytes. *Cardiovasc Res*. 2015;106(1):76–86.

22. https://github.com/raulbenitez/sparksimple

23. Marchena M, Echebarria B. Influence of the tubular network on the characteristics of calcium transients in cardiac myocytes. *PLoS One*. 2020;15(4):e0231056. https://doi.org/10.1371/journal.pone.0231056

24. Marchena M, Echebarria B. Computational model of calcium signaling in cardiac atrial cells at the submicron scale. *Front Physiol*. 2018;9:1760. https://doi.org/10.3389/fphys.2018.01760

25. Richards MA, Clarke JD, Saravanan P, et al. Transverse tubules are a common feature in large mammalian atrial myocytes including human. *Am J Physiol Circ Physiol*. 2011;301(5):H1996–H2005.

26. Shen X, van den Brink J, Hou Y, et al. 3D dSTORM imaging reveals novel detail of ryanodine receptor localization in rat cardiac myocytes. *J Physiol*. 2019;597(2):399–418.

27. https://github.com/blas71/sparks

28. Chelu MG, Sarma S, Sood S, et al. Calmodulin kinase II-mediated sarcoplasmic reticulum Ca2+ leak promotes atrial fibrillation in mice. *J Clin Invest*. 2009;119(7):1940–1951.

29. Ohkusa T, Ueyama T, Yamada J, et al. Alterations in cardiac sarcoplasmic reticulum Ca2+ regulatory proteins in the atrial tissue of patients with chronic atrial fibrillation. *J Am Coll Cardiol*. 1999;34(1):255–263.

30. Sun H, Gaspo R, Leblanc N, Nattel S. Cellular mechanisms of atrial contractile dysfunction caused by sustained atrial tachycardia. *Circulation*. 1998;98(7):719–727.

31. Nolla-Colomer C, Casabella-Ramon S, Jimenez-Sabado V, et al. β2-adrenergic stimulation potentiates spontaneous calcium release by increasing signal mass and co-activation of ryanodine receptor clusters. *Acta Physiol*. 2022;234(4):e13736. https://doi.org/10.1111/apha.13736

32. Sheehan KA, Zima AV, Blatter LA. Regional differences in spontaneous Ca $^{2+}$ spark activity and regulation in cat atrial myocytes. *J Physiol*. 2006;572(Pt 3):799–809.

33. Bosch R, Zeng X, Grammer JB, Popovic K, Mewis C, Kühlkamp V. Ionic mechanisms of electrical remodeling in human atrial fibrillation. *Cardiovasc Res*. 1999;44(1):121–131.

34. Van Wagoner DR. Electrophysiological remodeling in human atrial fibrillation. *Pacing Clin Electrophysiol*. 2003;26(7 Pt 2):1572–1575.

35. Dobrev D, Wehrens XHT. Calcium-mediated cellular triggered activity in atrial fibrillation. *J Physiol*. 2017;595(12):4001–4008.

36. Molina CE, Llach A, Herraiz-Martínez A, et al. Prevention of adenosine A2A receptor activation diminishes beat-to-beat alternation in human atrial myocytes. *Basic Res Cardiol*. 2016;111(1):5. https://doi.org/10.1007/s00395-015-0525-2

KEY WORDS **atrial fibrillation, human atrial myocyte, ryanodine receptor, sarcoplasmic reticulum, transient inward currents**

APPENDIX **For supplemental videos, figures, and a table, please see the online version of this paper.**